Effect of Gap Width on the Flame Propagation in a Millimeter-scale Closed Chamber

Jiepeng Huo [1, 2], Hang Su [1, 2], Liqiao Jiang [1], Xiaohan Wang [1], Daiqing Zhao [1 *]
[1] CAS Key Laboratory of Renewable Energy, Guangzhou Institute of Energy Conversion, Chinese Academy of Sciences, Guangzhou 510640, China
[2] University of Chinese Academy of sciences, Beijing 100049, China

1 Introduction

With great improvement of MEMS (Micro-electromechanical Systems) technologies, the fabrication and assembly of micro-engines have got fast development. However, in scale-down combustion chambers, the flame propagation has some limitations due to the flow field confinement and the sensitivities to the wall conditions [1]. Such limits have become the bottleneck of the miniaturization of engines. The propagation characteristics of premixed flames in millimeter-scale spaces are of great interest since they are relevance to the design of the combustion chambers of gas turbines and internal combustion engines [2].

Numerous experimental and numerical studies have been conducted in open channels in which the flame acceleration [3,4] and the effects of conductive heat losses [5] are mostly concerned. Wu and Wang [4] found that the flame accelerates earlier in smaller tubes, varied from 0.5 mm to 3.0 mm, suggesting that shorter time is required for the flame spread throughout a narrower combustion chamber. However, for a specific cooling condition, the intensity of the heat loss is proportional to the surface-area-to-volume ratio which increases with the reduction of the channel width. And it is known that the flame would decelerate or even become unsustainable for the existence of sufficient large volumetric heat loss. This indicates that there is an appropriate width resulting in the largest flame propagation velocity. However, few experimental data about the flame speed in closed chambers of millimeter scale is reported.

In this work, experimental and numerical study on the flame propagation phenomenon in a millimeter-scale closed chamber are presented. A narrow closed disc-shape chamber of which the gap width varies from 2 mm to 5 mm is constructed. The flame is ignited at the center under ambient pressure and temperature. Then the flame front propagates outward to the closed rim of the cylinder space. Considering that n-butane can be potentially used as a major fuel of miniature engines due to its great heat release rate and short ignition delay time,the n-butane/air mixture is used as the reactant. In order to provide an insight into the interaction of flame and the spatial scale, two-dimension transient numerical simulations are carried out to address the problem.

Correspondence to: Daiqing Zhao, Zhaodq@ms.giec.ac.cn

2 Experimental Setup

The millimeter-scale optical chamber is of 150 mm in diameter, assembled with a concave quartz plate and a convex one, as shown in Figure 1. The gap width H is set to 2.0 mm, 3.0 mm and 5.0 mm respectively in the present experiments by adjusting the bolts and the shims between the quartz plates. Stoichiometric premixed n-butane/air mixture is fed into the chamber under ambient pressure and temperature. The mixture is ignited by spark electrodes made by a double-orifice ceramic tube passing through two tungsten wires. The chamber is placed horizontally to avoid the influence of buoyancy. After the ignition, the transient flame propagating process are recorded by a high-speed CCD camera, of which the exposure time is fixed at 196.6 μs and the recorded speed is 5000 frames per second. More detailed description on the experimental procedures and corresponding uncertainties can be referred to Ref.[6].

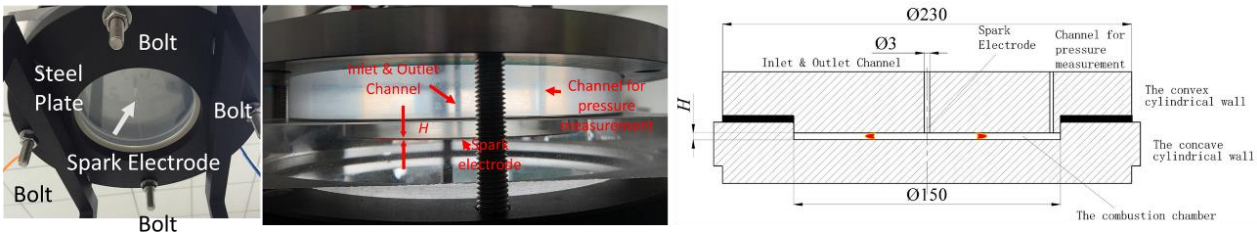

Figure 1. The structure and geometries of the disk-shape millimeter-scale closed chamber

Take the case of H=3.0 mm for example, the images of flame-front development captured by the camera are shown in Figure 2. Since the chamber diameter is much larger than the gap width, the flame front can be considered as a two-dimension expansion due to the configuration. Thus the radius of a circle which has the same enclosed area of the flame front is defined as the flame front location r_f in the radial direction. Then the flame front propagating velocity u_f can be obtained by calculating the increasing rate of r_f, namely dr_f/dt. Note that cellular structures of the flame are formed at the time of 25 ms, but it has been demonstrated that they have small influences on the flame speed which mainly depends on the local flow velocity [6].

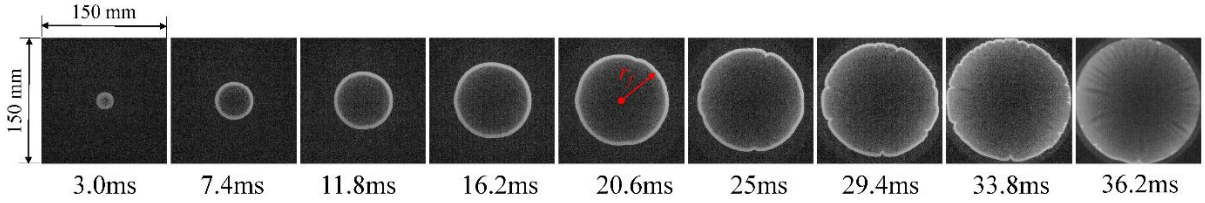

Figure 2. The images of flame-front development for H=3.0 mm

3 Computational method

For better understanding of the flame dynamics inside the chamber, central cross section was adopted as the computational domain in a two-dimensional numerical simulation. According to the experimental data, the flame front propagation speed is no more than 10 m/s, thus the corresponding Reynolds number is smaller than 500 resulting in laminar flow along the entire chamber. It has been demonstrated that laminar flame propagation phenomenon inside a confined channel can be successfully reproduced using two-dimensional transient model [7]. In this study, commercial software FLUENT was used to simulate such laminar reacting flow.

The schematic of the computational domain which is considered as an axisymmetric space and the types of boundaries are shown in Figure 3. Uniform structured grids are adopted in the domain of 75 mm×H which

depends on the cases. Structured square grids adapted to the gradient of temperature with three-level refinement were adopted in the simulations. The grid size is 50 μm×50 μm and the time step is 2 μs. In addition, one-step irreversible reaction mechanism is applied for n-butane/air reaction,

$$C_4H_{10}+6.5(O_2+3.76N_2)\rightarrow 4CO_2+5H_2O+24.44N_2, \quad (1)$$

$$\omega(\text{kmol/m}^3\text{-s})=9.841\times10^9\exp[(1.256\times10^8\,\text{J/kmol})/RT]\times C_{\text{N-butane}}^{0.15}C_{\text{Oxygen}}^{1.6}, \quad (2)$$

where R is the gas constant (J/kmol-K) and the concentrations are in units of kmol/m^3. It was adjusted to match the laminar flame speed s_L of 40.8 cm/s at stoichiometry and 1 atm for the premixed n-butane/air mixture, calculated by CHEMKIN-Pro with the detailed mechanism for C_1-C_4 hydrocarbons, USC-Mech II [8].

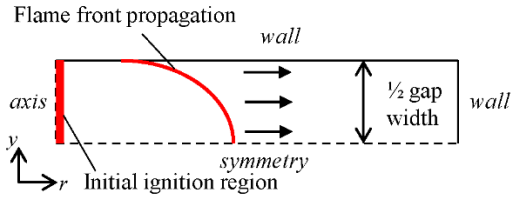

Figure 3. The schematic of the computational domain and the types of boundaries

The n-butane/air mixture was ignited by a small region in the center of the volume filled with burned gases. Adiabatic flame temperature and fractions of hot combustion products corresponding to the charged mixture were patched to the ignition region, size of 0.4 mm × H. The initial temperature and pressure of the system is 300 K and 1 atm. Gravity is neglected. It is worth noting that the specific heat capacity of quartz wall in the experiment is much larger than the total reaction heat of the mixture since the volume of millimeter-scale gap is extremely small. So that the boundary condition of the chamber wall is set as isothermal and the temperature of the wall T_w is also 300 K.

4 Results and Discussions

4.1 Validation of the simulation

The simulation results about the flame front location r_f various with time have good agreements with the counterparts obtained by experimental measure, as shown in Figure 4. The numerical results yield sligtly faster flame propagating velocities than experimental ones, probably due to the adoption of one-step global reaction mechanism which neglects all intermediate products during the reaction. Actually, an amount of several stable intermediate species (e.g. CO and H_2) can be generated in the vicinity of low-temperature wall due to incomplete combustion. It leads to a decrease of reaction rate across the flame front and therefore a slower propagation. Additionally, since the Markstein number of stoiometric n-butane/air mixure is positive [9], large curvature in the early stage of flame progation leads a reduction of buring velocity comtributing large discrepancy at early time. However, this effect cannot be captured by the 2-D simulation in this work.

It is interesting to find that both the experimental and numerical results indicates that the flame propagation velocity has non-monotonic relation with the gap width and it becomes largest for H=3.0 mm. In the early stage of the flame propagation after ignition, the velocities u_f are close to each other until the flame front reach half the gap radius. It is a bifurcation point where u_f for H= 2.0 mm drops significantly while u_f for H= 3.0 mm gradually surpasses the counterpart for H= 5.0 mm. These results reveal that the flame

propagation in a closed chamber is significantly affected by the gap width. This influence of gap width will be elucidated using the simulation data in the following discussions.

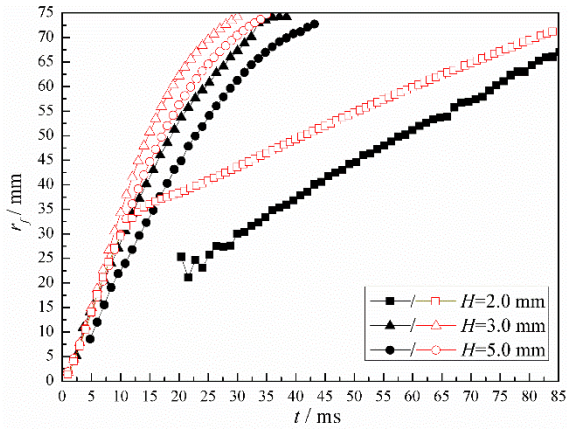

Figure 4. Time histories of flame front location r_f obtained by experiment (black solid) and numerical simulation (red hollow)

4.2 Flame Propagation in the Gap of H=2.0 mm

The temperature profiles along the symmetry of the simulation model are shown in Figure 5(a). It is found that the conductive heat loss to the cold wall has significant impact on the temperature of burned gas, leading to apparent decreases away from the flame fronts. In addition, the flame temperatures are almost identical with time, indicating that the heat release from the fuel consumption largely compensates the thermal loss. The comparison between the transient wall heat flux and the total heat release of reactions is shown in Figure 5(b). Note that in the vicinity of the above-mentioned bifurcation point of u_f for H=2.0 mm, both of them reduce and the wall heat flux almost equals to the heat release and this is the time of the slow down of flame propagation. It implies that after early stage of expansion, the heat loss from the burned gas to the wall approaches to certain degree that weaken the reaction rate across the flame front. And after self-regulation of the flame, the flame front moves constantly with a speed of approximately 56 cm/s, close to the laminar flame speed.

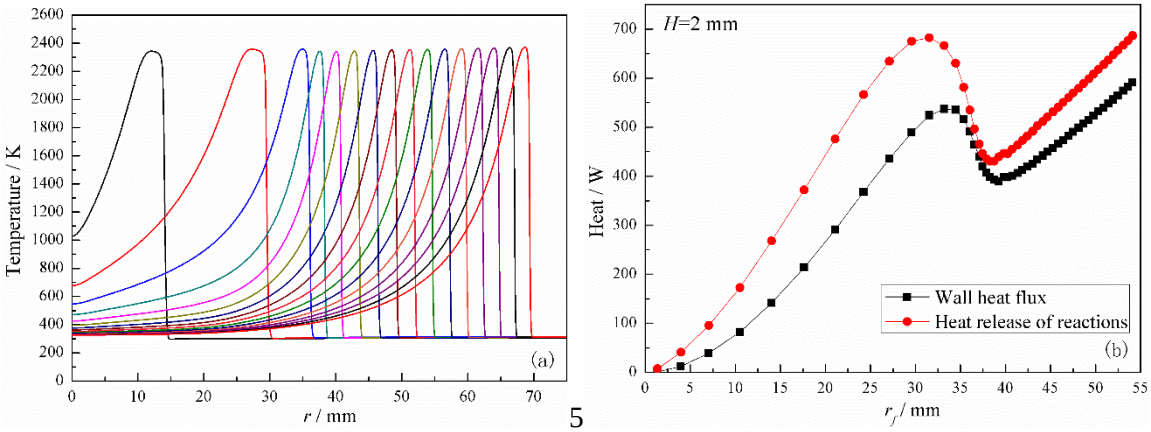

Figure 5. (a) Temperature profiles along the symmetry for the time from 5 ms to 80 ms. The time interval is 5 ms. (b) The dependence of wall heat flux and heat release of reactions on flame front locations r_f

Figure 6 demonstrates that most of the reaction heat compensates the thermal loss for the case of H=2.0 mm. The corresponding pressure profile hardly increase compared with the cases for larger gaps. Therefore, the slowest speed of the flame for H=2.0 mm mainly attributes to the thermal loss.

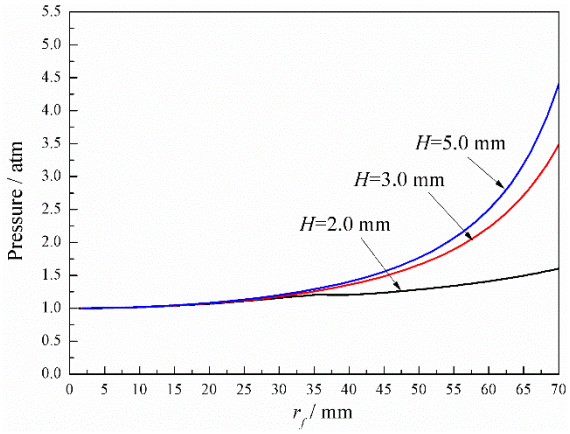

Figure 6. The pressure dependence of the cases for different gap width on flame front locations r_f

4.3 Flame Propagation in the Gap of H=3.0 mm and H=5.0 mm

The flame-shape evolution profiles for the cases of H=3.0 mm and H=5.0 mm are shown in Figure 7. One finds that their flame front patterns are different. For H=3.0 mm, finger-shape curved flame fronts due to thermal expansion of the burned gas and lateral confinement are developed, which enlarge the flame surface area. While for H=5.0 mm, the flame fronts are only distorted near the boundary at first. When the flame approaches r_f=30 mm, inverted flame fronts are exhibited. It indicates that for larger gaps, lateral confinement has less influence on the flame resulting in less elongate flame shapes.

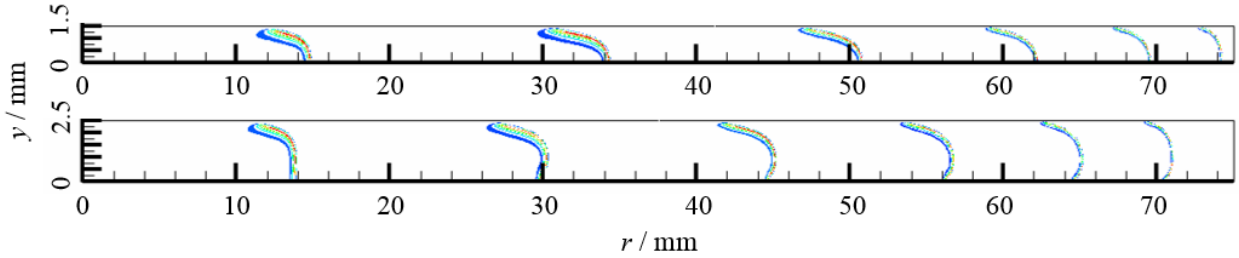

Figure 7. Composite of reaction rates at the flame front at selected times (t=5 ms, 10 ms, 15 ms, 20 ms, 25 ms and 30 ms) for the cases of H=3.0 mm and H=5.0 mm

Here, we define a dimensionless parameter ε to indicate the extent of flame straining,

$$\varepsilon = \frac{A_f}{2\pi r_f H} = \frac{2}{H}\int_{r_w}^{r_f} \frac{r}{r_f}\sqrt{1+\left(\frac{\mathrm{d}y}{\mathrm{d}r}\right)^2}\,\mathrm{d}r, \tag{3}$$

where A_f is the transient area of the flame surface, obtained by integrating the points which have the largest temperature derivation along the streamlines, r_f and r_w are the locations of the flame surface in the gap center and near the wall. The parameter ε refers to the surface area stretch ratio of the flame front. Figure 8 shows that ε for H=5.0 mm is smaller than that of H=3.0 mm. It is known that the flame acceleration is related to the flame straining which increases the reaction intensity. Therefore, a relatively slower propagation for H=3.0 mm are observed both experimentally and numerically. Note that it may not be a generalized result since flame

acceleration is coupled with geometries, reactant properties and initial thermal conditions. These complex impacts will be investigated in a future study.

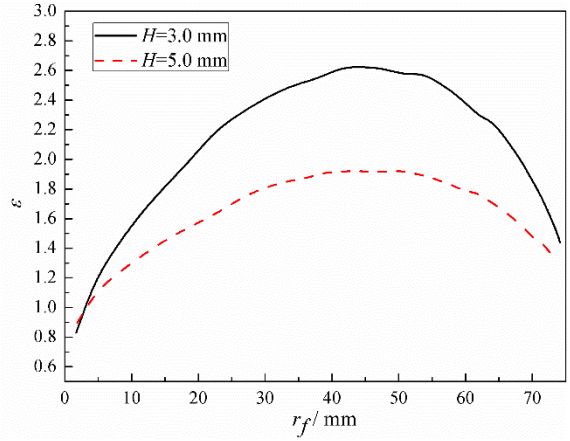

Figure 8. The ε evolution with r_f for H=3.0 mm and H=5.0 mm

5 Conclusions

Both experimental measure and numerical investigation find that flame propagation velocity in a closed millimeter-scale chamber is of great sensitive to the gap widths. Due to the combined effect of thermal expansion and heat loss of burned gas and lateral confinement of the chamber, there is a non-monotonic relation between the flame propagation velocity and the gap width. The optimal width is 3.0 mm. For narrower gaps, heat loss becomes dominant,while flame staining has a significant effect for larger gaps.

References

[1] Sher E. and Sher I. (2011) Theoretical limits of scaling-down internal combustion engines. Chem. Eng. Sci., 66, 260-267.
[2] Ju Y. and Maruta K. (2011) Microscale combustion: Technology development and fundamental research. Prog. Energy Combust. Sci., 37, 669-715.
[3] Wu M.H. and Kuo W.C. (2013) Accelerative expansion and ddt of stoichiometric ethylene/oxygen flame rings in micro-gaps. Proc. Combust. Instit., 34, 2017-2024.
[4] Wu M.H. and Wang C.Y. (2011) Reaction propagation modes in millimeter-scale tubes for ethylene/oxygen mixtures. Proc. Combust. Instit., 33, 2287-2293.
[5] Daou J. and Matalon M. (2002) Influence of conductive heat-losses on the propagation of premixed flames in channels. Combust. Flame, 128, 321-339.
[6] Jiang L.Q, Su H., Huo J.P., Li X., Yang H.L. and Zhao D.Q. (2018) Experimental Study on Propane/Air Flame Propagation Characteristics in a Disc-Like Gap Chamber. Combust. Sci. Technol., https://doi.org/10.1080/00102202.2018.1516647.
[7] Karlin V., Makhviladze G., Roberts J. and Melikhov V.I. (2000) Effect of lewis number on flame front fragmentation in narrow closed channels. Combust. Flame, 120, 173-187.
[8] Wang H., You X.Q., Joshi A.V., Davis A.G., Laskin A., Egolfopoulos F. and Law C.K. (2007) Usc mech version ii. High-temperature combustion reaction model of h2/co/c1-c4 compounds. Http://ignis.Usc.Edu/usc_mech_ii.Htm.
[9] Bechtold J.K. and Matalon M. (2001) The Dependence of the Markstein Length on Stoichiometry. Combust. Flame, 127:1906–1913.